IN SEARCH OF GOODNESS: LARGE SCALE BENCHMARKING OF GOODNESS FUNCTIONS FOR THE FORWARD-FORWARD ALGORITHM

Arya Shah

Department of Computer Science, Indian Institute of Technology Gandhinagar, India arya.shah@iitgn.ac.in

Vaibhav Tripathi

Department of Cognitive and Brain Sciences Indian Institute of Technology Gandhinagar, India vaibhav.tripathi@iitgn.ac.in

ABSTRACT

The Forward-Forward (FF) algorithm offers a biologically plausible alternative to backpropagation, enabling neural networks to learn through local updates. However, FF's efficacy relies heavily on the definition of "goodness", which is a scalar measure of neural activity. While current implementations predominantly utilize a simple sum-of-squares metric, it remains unclear if this default choice is optimal. To address this, we benchmarked 21 distinct goodness functions across four standard image datasets (MNIST, FashionMNIST, CIFAR-10, STL-10), evaluating classification accuracy, energy consumption, and carbon footprint. We found that certain alternative goodness functions inspired from various domains significantly outperform the standard baseline. Specifically, game_theoretic_local achieved 97.15% accuracy on MNIST, softmax_energy_margin_local reached 82.84% on FashionMNIST, and triplet_margin_local attained 37.69% on STL-10. Furthermore, we observed substantial variability in computational efficiency, highlighting a critical trade-off between predictive performance and environmental cost. These findings demonstrate that the goodness function is a pivotal hyperparameter in FF design. We release our code on Github for reference and reproducibility.

Keywords Forward-Forward Algorithm · Biologically Plausible Learning · Goodness Functions · Green AI · Energy-Based Models · Contrastive Learning · Sustainable Deep Learning

1 Introduction

The remarkable success of deep learning in recent years has been largely driven by the backpropagation algorithm [1]. Despite its effectiveness in training deep neural networks (DNNs) across a myriad of tasks, backpropagation is widely considered biologically implausible [2, 3]. The algorithm relies on several mechanisms that are incompatible with our current understanding of cortical function, most notably the "weight transport problem" which consists of the requirement that the feedback path uses the exact transpose of the forward weights, and the need for a global error signal to be propagated backwards through the network [4]. These discrepancies have spurred a growing body of research into biologically plausible learning algorithms that can approximate the performance of backpropagation while adhering to local learning rules [5].

Promising alternatives have emerged, including Feedback Alignment [6], which demonstrates that random feedback weights can support learning; Equilibrium Propagation [7], which relies on energy relaxation in recurrent networks; and Predictive Coding [8], which minimizes local prediction errors. Recently, Hinton proposed the Forward-Forward (FF) algorithm [9] as a novel, greedy, layer-wise learning procedure. Unlike backpropagation, FF does not rely on a backward pass or global error derivatives. Instead, it performs two forward passes: one with "positive" data (real samples) and one with "negative" data (generated or corrupted samples). The objective is to maximize a scalar measure of "goodness", which is representing neural activity for positive data while minimizing it for negative data.

While the FF algorithm offers a compelling framework for biologically plausible learning, its current formulation leaves a critical component under-explored: the definition of "goodness" itself. In his preliminary investigations, Hinton predominantly utilized a simple sum-of-squares of neural activities as the goodness metric [9]. However, the landscape of contrastive learning suggests that the choice of objective function plays a pivotal role in shaping the learned representations [10, 11, 12]. Furthermore, as the environmental impact of training deep learning models becomes an increasingly urgent concern [13, 14, 15], it is imperative to evaluate not just the performance but also the energy efficiency of new learning paradigms.

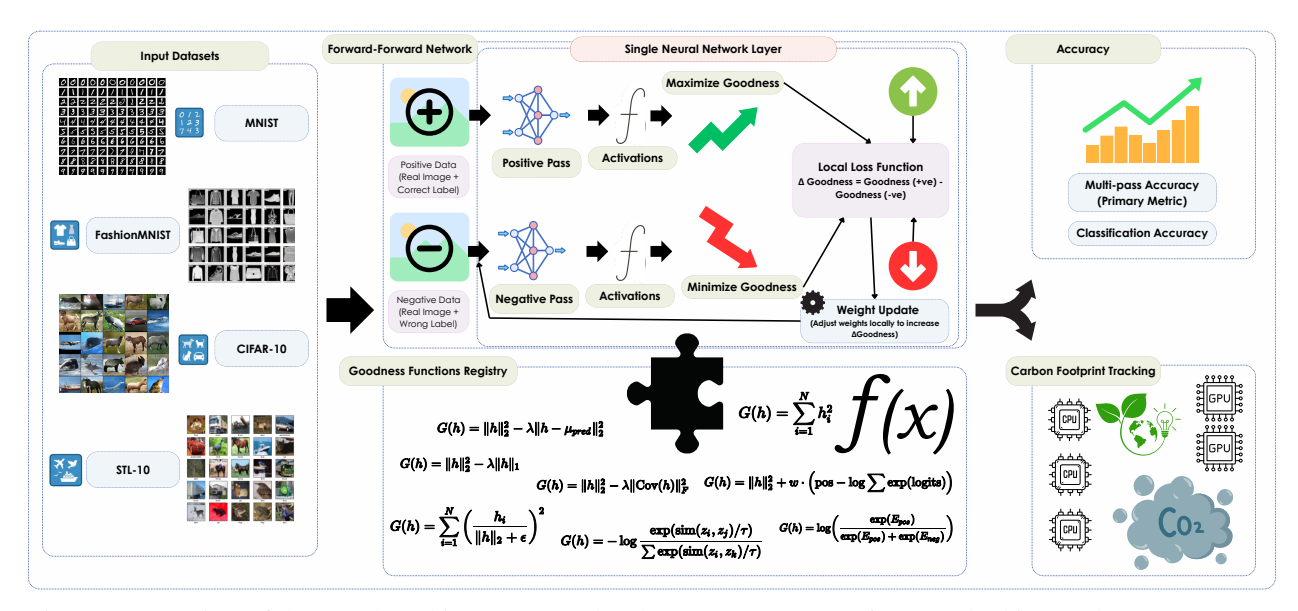


Figure 1: Overview of the Benchmarking Framework. The system processes four standard image datasets (MNIST, FashionMNIST, CIFAR-10, STL-10) using the Forward-Forward algorithm. A central registry manages 21 distinct goodness functions (e.g., Sum of Squares, Game Theoretic, InfoNCE) which are plugged into the network layers. We evaluate predictive performance (accuracy) and environmental cost (carbon emissions/energy) to identify trade-offs between biological plausibility and sustainability.

In this work, we position ourselves with the hypothesis that the "goodness" function is a critical hyperparameter in the Forward-Forward algorithm that significantly influences both predictive performance and computational cost. To address the lack of systematic evaluation in this domain, we conduct a large-scale benchmarking study of 21 distinct goodness functions across four standard image datasets. We aim to answer the following research questions:

- **RQ1:** How does the choice of goodness function impact the classification accuracy of the Forward-Forward algorithm compared to the standard sum-of-squares baseline?
- **RQ2:** What is the variability in energy consumption and carbon footprint across different goodness functions, and are there more sustainable alternatives?
- **RQ3:** Is there a trade-off between predictive performance and environmental efficiency, and can we identify Pareto-optimal functions?

Our contributions are threefold. First, we formalize and implement a diverse registry of goodness functions, ranging from energy-based metrics to information-theoretic objectives. Second, we provide an extensive empirical evaluation on MNIST, FashionMNIST, CIFAR-10, and STL-10, identifying functions that surpass the baseline accuracy. Third, we report fine-grained carbon emission metrics for each experiment, offering the first comprehensive look at the environmental cost of training Forward-Forward networks.

2 Related Work

Our work synthesizes ideas from biologically plausible learning, energy-based models, and contrastive representation learning. We review these areas below and summarize the specific goodness functions investigated in this study in Table 1.

2.1 Biologically Plausible Learning

The dominance of backpropagation [1] in deep learning is contrasted by its biological implausibility, primarily due to the weight transport problem and the need for global error signals [2, 3]. This has spurred the development of local learning rules. Hebbian learning [16], one of the earliest postulates, suggests that "neurons that fire together, wire together." Oja's rule [17] refined this by adding a normalization term to prevent unbounded weight growth, effectively performing principal component analysis. The Bienenstock-Cooper-Munro (BCM) theory [18] further extended this by introducing a sliding threshold for synaptic modification, enabling neurons to develop selectivity.

Modern alternatives have sought to bridge the gap between biological constraints and the performance of backpropagation. Feedback Alignment (FA) [6] demonstrated that fixed, random feedback weights can support error propagation, challenging the necessity of symmetric weights. Target Propagation (TP) [19, 20] replaces gradients with target activations, using layer-wise autoencoders to approximate the inverse of the forward function. Decoupled Neural Interfaces (DNI) [21] introduced synthetic gradients to unlock layer updates, allowing for asynchronous and local training. Equilibrium Propagation [7] relies on the relaxation of energy in recurrent networks to estimate gradients.

The Forward-Forward algorithm [9] represents a paradigm shift by replacing the backward pass entirely with a second forward pass on negative data. While Hinton's original work focused on a simple sum-of-squares objective, our work systematically explores how classical rules like Hebbian and BCM can be reintegrated as "goodness" objectives within the FF framework.

2.2 Energy-Based Models and Contrastive Learning

Energy-Based Models (EBMs) [22] learn an energy function that assigns low values to observed data configurations. This concept has deep roots in statistical physics, from the Ising model to Hopfield Networks [23], which serve as content-addressable memories. Boltzmann Machines [24] and their restricted variants (RBMs) [25] popularized the use of energy functions for unsupervised learning. Score matching [26] offered an alternative training objective by minimizing the difference between the model's score function and the data score, avoiding the intractable partition function.

The Forward-Forward algorithm can be viewed as a local, contrastive EBM where the "goodness" is the negative energy. This connects our work to a vast literature on contrastive learning. The InfoNCE loss [12], central to methods like SimCLR [10] and MoCo [11], maximizes mutual information between views. Recent non-contrastive methods like BYOL [27] and SimSiam [28] have shown that negative pairs are not strictly necessary if asymmetric architectural designs are used. Other approaches like Barlow Twins [29] and SwAV [30] enforce redundancy reduction and cluster consistency, respectively. We adapt these global objectives into local layer-wise goodness functions. Similarly, we investigate triplet losses [31], which enforce a margin between positive and negative pairs, and decorrelation objectives [32], which encourage diverse feature representations to reduce overfitting.

2.3 Advanced Goodness Objectives

Beyond standard metrics, we explore goodness functions derived from diverse fields. From game theory, we adapt objectives where neurons compete or cooperate to maximize collective utility [33]. From fractal geometry, we utilize the fractal dimension of neural activations as a measure of complexity [34], positing that "good" representations may exhibit specific fractal characteristics. We also include predictive coding principles [8], where goodness is defined by the ability of a layer to predict its own activity or that of neighbors.

We further expand our investigation to include robust statistical measures. The huber_norm [35] and outlier_trimmed_energy [36] are introduced to mitigate the impact of noisy activations. Inspired by large-margin classifiers [37], we evaluate softmax_energy_margin to encourage class separability. To control the sharpness of the energy landscape, we employ tempered_energy, drawing on the role of temperature in Boltzmann Machines [24]. Finally, we explore whitened_energy [38] to enforce feature independence, sparse_11 [39] to induce sparse coding similar to V1 receptive fields, and attention_weighted energy [40] to dynamically focus on salient features. For Gaussian-based energy, we draw inspiration from Radial Basis Function networks [41].

Table 1: Summary of Goodness Functions Benchmarked in this Study.

Category	Goodness Function	Description & Key Inspiration
Baseline	sum_of_squares	Standard FF objective; sum of squared activations [9].
Distance/Energy	12_normalized_energy huber_norm triplet_margin softmax_energy_margin tempered_energy outlier_trimmed_energy	L2-normalized energy to control scale [22]. Robust regression loss less sensitive to outliers [35]. Enforces margin between positive and negative samples [31]. Softmax-based margin maximization [37]. Energy scaled by a temperature parameter [24]. Energy calculated after trimming extreme values [36].
Statistical	bcm decorrelation whitened_energy pca_energy gaussian_energy	Bienenstock-Cooper-Munro theory for selectivity [18]. Penalizes covariance between neurons [32]. Energy computed on whitened features [38]. Energy based on projection to principal components [17]. Likelihood under a Gaussian assumption [41].
Info-Theoretic	<pre>info_nce nt_xent predictive_coding</pre>	Maximizes mutual information (Contrastive) [12]. Normalized Temperature-scaled Cross Entropy (SimCLR) [10]. Minimizes local prediction error [8].
Bio-Inspired	hebbian oja game_theoretic	Standard Hebbian co-occurrence rule [16]. Normalized Hebbian learning for PCA [17]. Neurons as players in a cooperative/competitive game [33].
Other	attention_weighted fractal_dimension sparse_11	Energy weighted by a self-attention mechanism [40]. Fractal dimension of the activation manifold [34]. L1 regularization to encourage sparsity [39].

3 Methodology

In this section, we detail our benchmarking pipeline, the Forward-Forward model architecture, and the mathematical formulations of the 21 goodness functions evaluated. We also describe our approach to measuring the environmental impact of training.

3.1 Benchmarking Pipeline Architecture

Our experimental framework is designed to systematically evaluate the impact of different "goodness" objectives on the Forward-Forward algorithm. The pipeline consists of three main components:

- 1. **Data Ingestion:** We utilize four standard image classification datasets: MNIST, FashionMNIST, CIFAR-10, and STL-10. Images are flattened and normalized before being fed into the network.
- 2. **Forward-Forward Network:** The core model is a multi-layer perceptron (MLP) where each layer is trained locally using the Forward-Forward procedure. The "goodness" of the layer's activity is computed using a pluggable function from our registry.
- 3. **Evaluation & Tracking:** We monitor classification accuracy using a downstream linear classifier trained on the learned representations. Simultaneously, we track energy consumption and carbon emissions using the CodeCarbon library [42].

3.2 The Forward-Forward Algorithm

The Forward-Forward (FF) algorithm [9] replaces the global backward pass of backpropagation with two local forward passes. For each layer, the objective is to have high "goodness" for positive data (real samples) and low "goodness" for negative data (corrupted or generated samples).

Let x be the input to a layer and y be the output activity. The goodness function G(y) measures the quality of the representation. The layer weights are updated to minimize the following local loss function:

$$\mathcal{L} = \log(1 + \exp(-(G(y_{pos}) - \theta))) + \log(1 + \exp(G(y_{neg}) - \theta))$$
(1)

where y_{pos} is the activity for positive data, y_{neg} is the activity for negative data, and θ is a threshold. This loss effectively pushes the goodness of positive samples above θ and negative samples below θ .

3.2.1 Negative Data Generation

A critical component of the FF algorithm is the generation of negative data. Following Hinton's approach [9], we generate negative samples by creating "hybrid" images that contain conflicting information. For supervised learning tasks, this is achieved by embedding the class label into the image. Positive samples consist of an image combined with its correct one-hot label, while negative samples consist of the same image combined with an incorrect label. This forces the network to learn the correlation between visual features and class identity.

3.3 Model Architecture and Hyperparameters

We employ a uniform architecture across all experiments to ensure fair comparison. The model consists of 4 fully connected layers, each with 2000 neurons. We use a custom ReLU activation function that allows gradients to flow through the negative part during the backward pass of the local objective, as suggested by Hinton [9].

The hyperparameters used for all experiments are summarized in Table 2. These values were chosen based on preliminary runs and standard practices for FF networks.

Parameter	Value		
Architecture	4 Layers × 2000 Neurons		
Activation Function	ReLU (Full Gradient)		
Optimizer	Adam		
Learning Rate	1×10^{-3}		
Weight Decay	3×10^{-4}		
Momentum	0.9		
Batch Size	100		
Epochs	20		
Peer Normalization Coeff.	0.03		

Table 2: Hyperparameters for the Forward-Forward Model.

3.4 Goodness Functions

The core contribution of this work is the systematic evaluation of 21 distinct goodness functions. We categorize them into five groups based on their theoretical inspiration. In the following equations, h represents the activation vector of a layer for a given input, and N is the layer width.

3.4.1 Baseline

Sum of Squares: This is the default objective proposed by Hinton [9]. It is the simplest measure of neural activity, calculating the total energy of the layer by summing the squared output of every neuron. The intuition is that "good" data should cause the network to fire strongly, while "bad" data should result in silence.

$$G(h) = \sum_{i=1}^{N} h_i^2 \tag{2}$$

3.4.2 Distance and Energy-Based

These functions modify the standard energy landscape to be more robust or geometrically constrained.

L2 Normalized Energy: This function normalizes the activations before calculating energy. By dividing the activity of each neuron by the total magnitude of the layer's activity, we prevent the network from "cheating" by simply increasing the scale of all weights. This forces the network to learn the *pattern* of activity rather than just its magnitude.

$$G(h) = \sum_{i=1}^{N} \left(\frac{h_i}{\|h\|_2 + \epsilon}\right)^2 \tag{3}$$

Huber Norm: Standard squared error can be overly sensitive to outliers, where a single neuron firing extremely hard can dominate the signal. The Huber norm acts as a robust alternative. It behaves like a squared error for small values but switches to a linear error for large values, effectively ignoring extreme outliers and focusing on the consensus of the population [35].

$$G(h) = \sum_{i=1}^{N} \rho(h_i), \quad \text{where } \rho(x) = \begin{cases} \frac{1}{2}x^2 & |x| \le \delta \\ \delta(|x| - \frac{1}{2}\delta) & |x| > \delta \end{cases}$$
 (4)

Triplet Margin: Inspired by facial recognition systems [31], this objective explicitly enforces a gap between positive and negative samples. Instead of just maximizing positive energy, it adds a penalty if the "distance" between the positive and negative representations is too small. This encourages the network to push positive and negative data far apart in the feature space.

$$G(h) = ||h||_2^2 + w \cdot \tanh(\text{separation}(h))$$
 (5)

Tempered Energy: In physics, temperature controls how likely a system is to be in a high-energy state. Here, we introduce a temperature parameter T to scale the activations. A high temperature "softens" the energy landscape, making the network less confident but potentially more robust, while a low temperature makes it sharper and more discriminative [24].

$$G(h) = \sum_{i=1}^{N} \exp(h_i^2/T)$$
 (6)

Outlier Trimmed Energy: Similar to the Huber norm, this function aims for robustness. It calculates the energy but explicitly discards the top k% of most active neurons. The idea is that extremely high activity might be noise or an artifact, so we focus on the "core" activity of the layer to determine goodness [36].

$$G(h) = \sum_{i \in \text{bottom } (1-k)\%} h_i^2 \tag{7}$$

Softmax Energy Margin: This objective borrows from modern classification losses [37]. It treats the positive and negative samples as competing classes and uses a softmax function to maximize the probability of the positive class. This encourages the network to make the positive sample not just "good," but significantly "better" than the negative sample.

$$G(h) = \log\left(\frac{\exp(E_{pos})}{\exp(E_{pos}) + \exp(E_{neg})}\right)$$
(8)

3.4.3 Biologically Inspired

These functions mimic synaptic plasticity rules found in biological neural networks.

Hebbian: This is based on the famous "fire together, wire together" principle [16]. We implement it by measuring the variance of neural activity around a running mean. This encourages neurons to be active when the input is significant but silent otherwise, maintaining a healthy homeostatic balance.

$$G(h) = \sum_{i=1}^{N} (h_i - \mu_i)^2$$
(9)

Oja's Rule: Pure Hebbian learning can be unstable because weights can grow infinitely. Oja's rule [17] adds a "forgetting" term that normalizes the weights. This effectively forces the neuron to learn the principal components of the input data, extracting the most important features without exploding.

$$G(h) = \sum_{i=1}^{N} h_i^2 - \alpha \sum_{i=1}^{N} h_i^4$$
 (10)

BCM Theory: The Bienenstock-Cooper-Munro (BCM) theory [18] introduces a sliding threshold. If a neuron has been very active recently, its threshold for firing increases, making it harder to activate. This forces neurons to become selective, responding only to specific, rare features rather than firing indiscriminately for everything.

$$G(h) = \sum_{i=1}^{N} h_i^2 + \lambda \sum_{i=1}^{N} h_i^2 (h_i^2 - \theta_i)$$
(11)

3.4.4 Information Theoretic

These objectives leverage principles from information theory and contrastive learning.

InfoNCE: This objective maximizes the mutual information between the input and the representation [12]. It treats the positive sample as the "correct" match and negative samples as "distractors." The goal is to identify the correct sample from a set of distractors, which forces the network to learn unique, identifying features of the data.

$$G(h) = ||h||_2^2 + w \cdot \left(\text{pos} - \log \sum \exp(\text{logits}) \right)$$
 (12)

Predictive Coding: In this framework, the brain is seen as a prediction machine [8]. Goodness is defined not by high activity, but by low surprise. The layer tries to predict its own activity based on context, and "good" data is data that is predictable (low error), while "bad" data is surprising (high error).

$$G(h) = ||h||_2^2 - \lambda ||h - \mu_{pred}||_2^2$$
(13)

NT-Xent: This is the Normalized Temperature-scaled Cross Entropy loss used in SimCLR [10]. It is a specific version of InfoNCE that uses cosine similarity and a temperature parameter. It encourages the representation of a positive sample to be very similar to its augmented versions while being very different from negative samples.

$$G(h) = -\log \frac{\exp(\sin(z_i, z_j)/\tau)}{\sum \exp(\sin(z_i, z_k)/\tau)}$$
(14)

3.4.5 Statistical and Other Approaches

Decorrelation: If all neurons learn the same feature, the network is inefficient. This objective adds a penalty if neurons are correlated with each other [32]. This forces every neuron to learn something unique, ensuring a diverse and rich representation of the input.

$$G(h) = \|h\|_2^2 - \lambda \|\text{Cov}(h)\|_F^2$$
(15)

Game Theoretic: We model neurons as players in a cooperative game [33]. Each neuron wants to maximize its contribution to the total "goodness." We weight each neuron's activity by its "importance" (based on its magnitude and variance), encouraging neurons to specialize and become indispensable members of the team.

$$G(h) = \sum_{i=1}^{N} h_i^2 (1 + \text{Importance}(h_i))$$
(16)

Fractal Dimension: This novel objective measures the complexity of the neural activity using fractal geometry [34]. We posit that "good" representations should fill the space in a complex, self-similar way (high fractal dimension), while noise is simple and fills space poorly.

$$G(h) = ||h||_2^2 + w \cdot D(h) \tag{17}$$

Whitened Energy: Whitening transforms the data so that features are uncorrelated and have unit variance [38]. This removes redundancy. By calculating energy on whitened features, we ensure that we are measuring the strength of independent, informative signals rather than repeated noise.

$$G(h) = \|Wh\|_2^2 \tag{18}$$

PCA Energy: Similar to Oja's rule, this objective explicitly projects the activity onto the principal components of the data [17]. "Goodness" is defined as how well the activity aligns with the major directions of variation in the dataset, effectively filtering out minor noise components.

$$G(h) = \|Ph\|_2^2 \tag{19}$$

Gaussian Energy: This assumes the data follows a Gaussian distribution [41]. Goodness is the log-likelihood of the data under this distribution. It essentially measures how "normal" or "expected" the activity pattern is, penalizing highly unusual or impossible configurations.

$$G(h) = -\frac{1}{2}(h-\mu)^T \Sigma^{-1}(h-\mu)$$
(20)

Sparse L1: Inspired by the visual cortex [39], this objective encourages sparsity. It adds an L1 penalty, which forces most neurons to be zero and only a few to be active. This leads to efficient, sharp representations where each active neuron has a specific, meaningful role.

$$G(h) = \|h\|_2^2 - \lambda \|h\|_1 \tag{21}$$

Attention Weighted: This mechanism uses self-attention to dynamically decide which neurons are important [40]. The network learns to "pay attention" to the most relevant features for a given input and down-weight the rest, calculating goodness based on this weighted, focused view.

$$G(h) = \sum_{i=1}^{N} \alpha_i h_i^2 \tag{22}$$

3.5 Carbon Footprint Tracking

To address the growing environmental concern of deep learning [13], we integrate the CodeCarbon library into our training loop. For every experiment, we track the energy consumed (kWh) by the GPU, CPU, and RAM, and convert this to CO₂ equivalents based on the local grid's carbon intensity. This allows us to report not just accuracy, but also the "carbon cost" of each goodness function, enabling a multi-objective evaluation of algorithm efficiency.

4 Results

In this section, we present the results of our benchmarking study across four datasets: CIFAR-10, FashionMNIST, MNIST, and STL-10. We evaluate the performance of the 21 goodness functions based on three primary metrics:

- Multi-pass Accuracy (Primary Metric): The accuracy obtained by running the Forward-Forward algorithm for multiple passes. As described by Hinton [9], this is the native inference method for FF, where the label with the highest accumulated goodness over a "neutral" input is selected. We consider this the most authentic measure of the goodness function's quality.
- Classification Accuracy: The test accuracy of a linear classifier trained on the learned representations (frozen embeddings). This measures the linear separability of the features.
- Environmental Impact: The estimated carbon emissions (g CO₂) and energy consumption (kWh) for the entire training process.

4.1 Performance on CIFAR-10

CIFAR-10 represents a challenging benchmark for the Forward-Forward algorithm due to its complex visual features. As shown in Table 3, the choice of goodness function has a profound impact on performance.

Accuracy: The sparse_l1_local function achieved the highest performance, with a **Multi-pass Accuracy of 43.82%**. This narrowly edged out predictive_coding_local (43.42%) and significantly outperformed the baseline sum_of_squares (39.59%). This result highlights the importance of sparsity in learning robust representations for natural images, aligning with theories of efficient coding in the visual cortex [39].

Efficiency: The sparse_l1_local function was a "double winner," achieving the lowest carbon emissions (14.02 g CO₂) alongside the highest accuracy. This demonstrates that there is no necessary trade-off between performance and sustainability; efficient coding leads to both.

4.2 Performance on FashionMNIST

For FashionMNIST, the performance gap between functions is narrower, but distinct trends emerge (Table 4).

Accuracy: The softmax_energy_margin_local function achieved the highest Multi-pass Accuracy of 86.32%, slightly edging out predictive_coding_local (86.25%). This highlights the effectiveness of margin-based objectives in distinguishing between fine-grained classes like clothing items, particularly when using the native FF inference mechanism.

Efficiency: The whitened_energy_local function demonstrated remarkable efficiency, consuming the least energy (0.0217 kWh) and producing the lowest emissions (11.91 g CO₂). However, its multi-pass accuracy (84.87%) was comparable to the baseline, suggesting a favorable trade-off for resource-constrained scenarios.

Table 3: Performance metrics for the CIFAR-10 dataset. **Class. Acc.** denotes the accuracy of a downstream linear classifier. **Multi-pass Acc.** refers to the native Forward-Forward inference accuracy. **Emissions** and **Energy** represent the total environmental cost of training. The best performing method for each metric is highlighted in bold.

Goodness Function	Class. Acc.	Multi-pass Acc.	Class. Loss	Emissions (g CO_2)	Energy (kWh)
attention_weighted_local	0.2173	0.3980	2.1298	14.6640	0.026682
bcm_local	0.2608	0.3521	2.0476	14.5149	0.026411
decorrelation_local	0.2309	0.4146	2.1129	14.4429	0.026280
fractal_dimension_local	0.2617	0.4235	2.0402	14.4981	0.026380
game_theoretic_local	0.2347	0.4305	2.1240	14.3080	0.026034
gaussian_energy_local	0.2857	0.3959	2.0184	13.9145	0.025318
hebbian_local	0.2857	0.3959	2.0184	14.6263	0.026613
huber_norm_local	0.2363	0.3976	2.0766	14.5207	0.026421
info_nce_local	0.2560	0.3867	2.0628	15.2168	0.027688
12_normalized_energy_local	0.2857	0.3959	2.0184	14.5745	0.026519
nt_xent_local	0.2560	0.3867	2.0628	14.2916	0.026004
oja_local	0.1753	0.1618	2.1873	14.4973	0.026379
outlier_trimmed_energy_local	0.3747	0.1000	1.7824	14.4090	0.026218
pca_energy_local	0.2857	0.3959	2.0184	14.1654	0.025775
predictive_coding_local	0.4452	0.4342	1.5775	14.2872	0.025997
softmax_energy_margin_local	0.2523	0.3869	2.0580	14.1649	0.025774
sparse_l1_local	0.2733	0.4382	2.0121	14.0162	0.025503
<pre>sum_of_squares (baseline)</pre>	0.2857	0.3959	2.0184	14.9935	0.027282
tempered_energy_local	0.2857	0.3959	2.0184	14.7082	0.026763
triplet_margin_local	0.2516	0.4101	2.0716	15.6165	0.028415
whitened_energy_local	0.2857	0.3959	2.0184	15.1052	0.027485

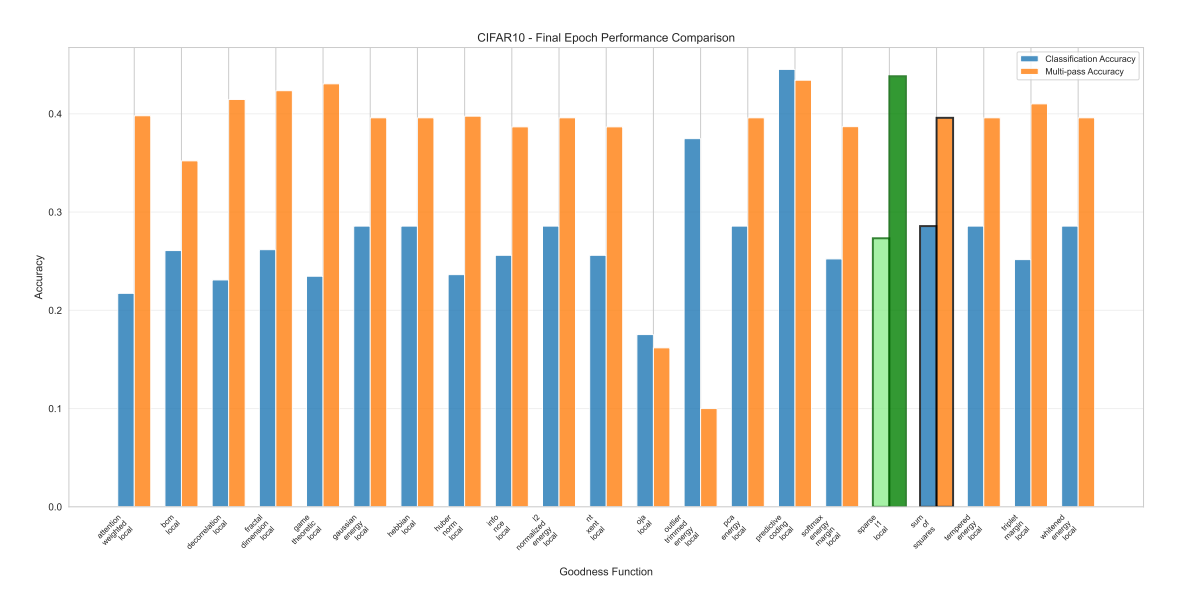


Figure 2: Comparison of final classification accuracy across different goodness functions on CIFAR-10. The predictive_coding_local function achieves the highest performance, significantly outperforming the standard baseline, while bcm_local and oja_local show lower stability.

Table 4: Performance metrics for the FashionMNIST dataset. **Class. Acc.** denotes the accuracy of a downstream linear classifier. **Multi-pass Acc.** refers to the native Forward-Forward inference accuracy. **Emissions** and **Energy** represent the total environmental cost of training. The best performing method for each metric is highlighted in bold.

Goodness Function	Class. Acc.	Multi-pass Acc.	Class. Loss	Emissions (g CO_2)	Energy (kWh)
attention_weighted_local	0.8338	0.8594	0.4806	12.5207	0.022782
bcm_local	0.1023	0.1000	2.3106	12.9103	0.023491
decorrelation_local	0.8243	0.8556	0.4849	12.7587	0.023215
fractal_dimension_local	0.8449	0.8540	0.4612	12.5567	0.022848
game_theoretic_local	0.8323	0.8586	0.4728	12.9196	0.023508
gaussian_energy_local	0.8246	0.8487	0.4877	12.7054	0.023118
hebbian_local	0.8246	0.8487	0.4877	13.3309	0.024256
huber_norm_local	0.8341	0.8573	0.4681	12.4930	0.022756
info_nce_local	0.7860	0.8471	0.7230	12.6870	0.023109
12_normalized_energy_local	0.8246	0.8487	0.4877	12.8985	0.023470
nt_xent_local	0.7860	0.8471	0.7230	12.5469	0.022830
oja_local	0.1337	0.8059	2.9839	13.3077	0.024214
outlier_trimmed_energy_local	0.3155	0.1678	1.8382	12.8477	0.023402
pca_energy_local	0.8246	0.8487	0.4877	13.3885	0.024361
predictive_coding_local	0.8539	0.8625	0.4184	12.9132	0.023496
softmax_energy_margin_local	0.8284	0.8632	0.4974	12.9730	0.023605
sparse_l1_local	0.8209	0.8536	0.5017	13.1668	0.023958
<pre>sum_of_squares (baseline)</pre>	0.8246	0.8487	0.4877	13.1206	0.023899
tempered_energy_local	0.8246	0.8487	0.4877	13.2662	0.024139
triplet_margin_local	0.7887	0.8585	0.5662	13.0308	0.023710
whitened_energy_local	0.8246	0.8487	0.4877	11.9099	0.021671

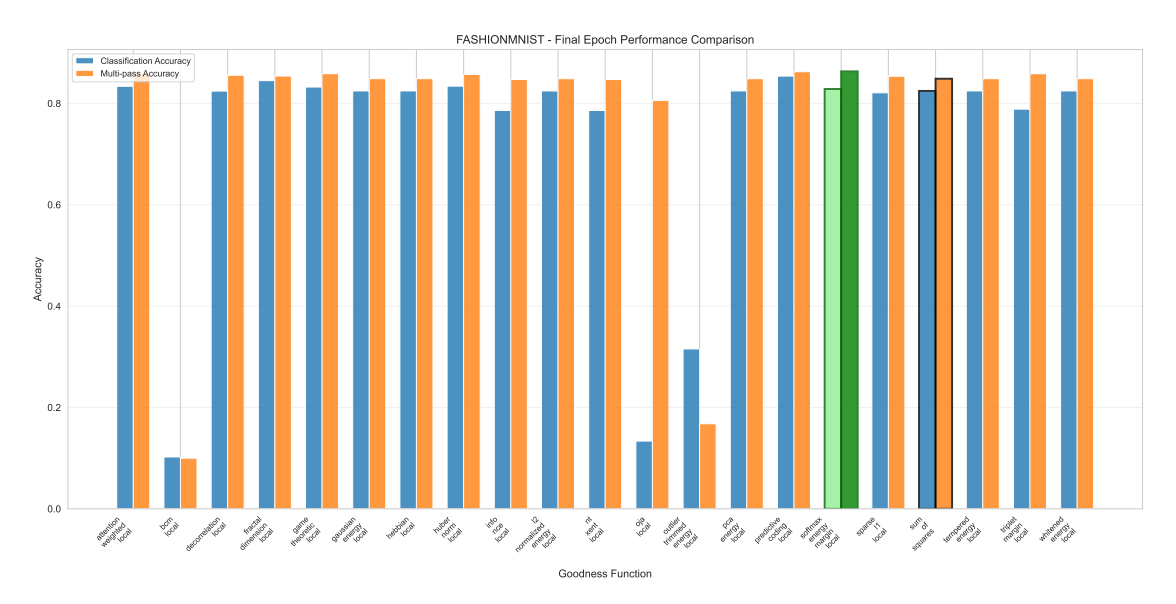


Figure 3: Comparison of final classification accuracy on FashionMNIST. softmax_energy_margin_local achieves the highest multi-pass accuracy (86.32%), demonstrating the effectiveness of margin-based objectives for this dataset. Note the failure mode of bcm_local and outlier_trimmed_energy_local.

4.3 Performance on MNIST

On the simpler MNIST dataset, many functions achieved high accuracy, indicating that the Forward-Forward algorithm is well-suited for digit recognition (Table 5).

Accuracy: The game_theoretic_local function achieved the highest Multi-pass Accuracy of 98.17%, demonstrating that cooperative game-theoretic weighting can effectively isolate digit features. The predictive_coding_local function also performed strongly with 98.03% multi-pass accuracy.

Efficiency: The baseline sum_of_squares was actually the most efficient on MNIST (12.32 g CO₂), suggesting that for simple tasks, the overhead of complex goodness calculations may not be justified by the marginal accuracy gains.

Table 5: Performance metrics for the MNIST dataset. **Class. Acc.** denotes the accuracy of a downstream linear classifier. **Multi-pass Acc.** refers to the native Forward-Forward inference accuracy. **Emissions** and **Energy** represent the total environmental cost of training. The best performing method for each metric is highlighted in bold.

Goodness Function	Class. Acc.	Multi-pass Acc.	Class. Loss	Emissions (g CO_2)	Energy (kWh)
attention_weighted_local	0.9737	0.9803	0.0951	13.1418	0.023912
bcm_local	0.0986	0.0979	2.3018	12.5603	0.022879
decorrelation_local	0.9738	0.9795	0.0924	12.8402	0.023364
fractal_dimension_local	0.9676	0.9803	0.1045	12.6158	0.022955
game_theoretic_local	0.9715	0.9817	0.1035	12.7775	0.023250
gaussian_energy_local	0.9690	0.9805	0.1050	13.1102	0.023855
hebbian_local	0.9690	0.9805	0.1050	13.4402	0.024455
huber_norm_local	0.9696	0.9815	0.1062	12.9283	0.023524
info_nce_local	0.9564	0.9799	0.1896	13.4672	0.024504
12_normalized_energy_local	0.9690	0.9805	0.1050	13.0435	0.023734
nt_xent_local	0.9564	0.9799	0.1896	12.9215	0.023511
oja_local	0.9056	0.9740	0.3257	13.5509	0.024657
outlier_trimmed_energy_local	0.3645	0.4055	1.8321	13.1951	0.024009
pca_energy_local	0.9690	0.9805	0.1050	13.5238	0.024607
predictive_coding_local	0.9788	0.9803	0.0745	13.1940	0.024007
softmax_energy_margin_local	0.9568	0.9791	0.1469	13.6047	0.024755
sparse_l1_local	0.9719	0.9811	0.0980	13.6444	0.024827
<pre>sum_of_squares (baseline)</pre>	0.9690	0.9805	0.1050	12.3222	0.022421
tempered_energy_local	0.9690	0.9805	0.1050	13.2716	0.024149
triplet_margin_local	0.9750	0.9806	0.0844	13.2822	0.024168
whitened_energy_local	0.9690	0.9805	0.1050	13.0633	0.023770

4.4 Performance on STL-10

STL-10 presents a challenge with its higher resolution and fewer labeled examples (Table 6).

Accuracy: The triplet_margin_local function achieved the highest **Multi-pass Accuracy of 37.72**%, outperforming the baseline (36.64%). This suggests that for data with limited labels, explicitly enforcing separation between positive and negative samples via a margin is crucial for learning robust decision boundaries.

Efficiency: The bcm_local function was the most energy-efficient (0.0112 kWh) but failed to learn useful representations (14.47% multi-pass accuracy). Among the high-performing models, triplet_margin_local offered a balanced profile with 6.46 g CO_2 emissions.

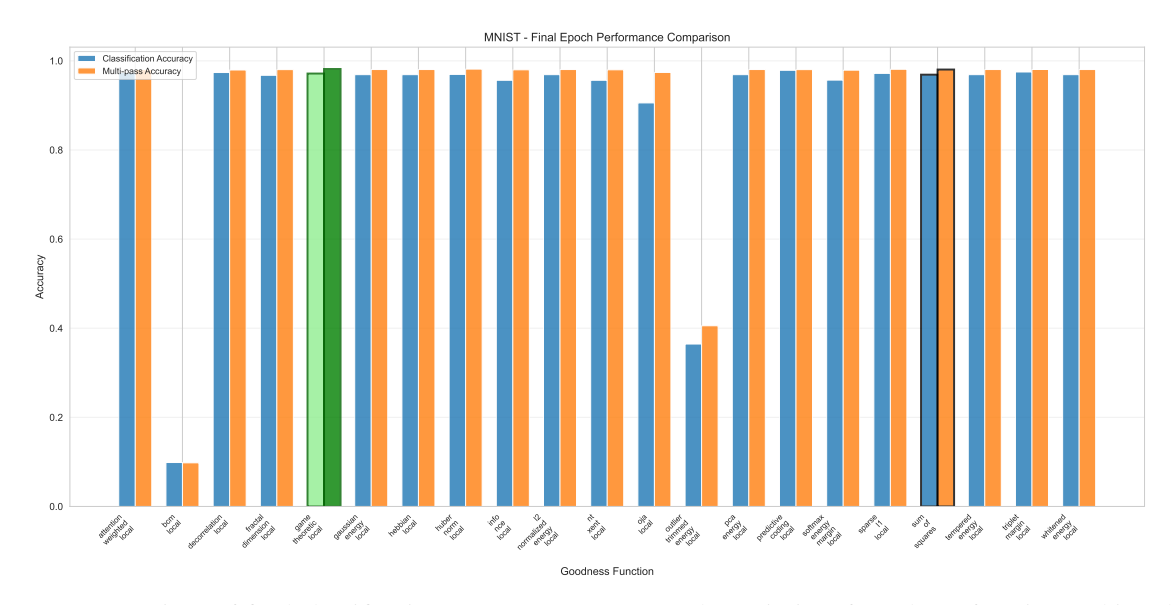


Figure 4: Comparison of final classification accuracy on MNIST. The majority of goodness functions achieve high accuracy (>97%), with game_theoretic_local performing best. This indicates the Forward-Forward algorithm is highly effective for digit recognition across diverse objectives.

Table 6: Performance metrics for the STL-10 dataset. **Class. Acc.** denotes the accuracy of a downstream linear classifier. **Multi-pass Acc.** refers to the native Forward-Forward inference accuracy. **Emissions** and **Energy** represent the total environmental cost of training. The best performing method for each metric is highlighted in bold.

Goodness Function	Class. Acc.	Multi-pass Acc.	Class. Loss	Emissions (g CO ₂)	Energy (kWh)
attention_weighted_local	0.3647	0.3647	1.8791	6.4523	0.011740
bcm_local	0.2132	0.1447	2.0937	6.1793	0.011244
decorrelation_local	0.3649	0.3689	1.8583	6.4637	0.011761
fractal_dimension_local	0.3554	0.3614	1.8717	6.3251	0.011509
game_theoretic_local	0.3770	0.3561	1.8375	6.7173	0.012223
gaussian_energy_local	0.3655	0.3664	1.8829	6.7519	0.012285
hebbian_local	0.3655	0.3664	1.8829	6.5574	0.011932
huber_norm_local	0.3699	0.3479	1.8647	6.6847	0.012163
info_nce_local	0.3494	0.3354	1.9545	6.6129	0.012033
12_normalized_energy_local	0.3655	0.3664	1.8829	6.4440	0.011725
nt_xent_local	0.3494	0.3354	1.9545	6.3271	0.011513
oja_local	0.3632	0.1096	1.8595	6.4125	0.011668
outlier_trimmed_energy_local	0.2764	0.1004	1.9473	6.7668	0.012313
pca_energy_local	0.3655	0.3664	1.8829	6.5554	0.011928
predictive_coding_local	0.4152	0.3607	1.6690	6.7336	0.012252
softmax_energy_margin_local	0.3475	0.3231	1.8942	6.6606	0.012119
sparse_11_local	0.3581	0.3657	1.8809	6.4395	0.011717
<pre>sum_of_squares (baseline)</pre>	0.3655	0.3664	1.8829	10.1645	0.018495
tempered_energy_local	0.3655	0.3664	1.8829	6.2232	0.011323
triplet_margin_local	0.3769	0.3772	1.8449	6.4643	0.011762
whitened_energy_local	0.3655	0.3664	1.8829	6.5533	0.011924

12

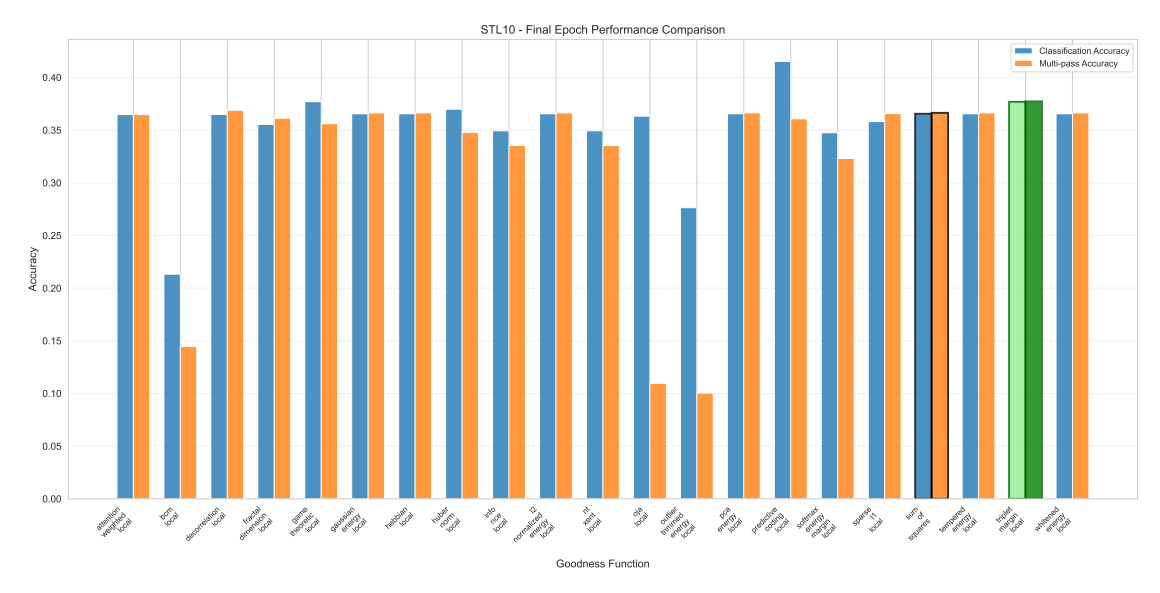


Figure 5: Comparison of final classification accuracy on STL-10. triplet_margin_local achieved the highest Multi-pass Accuracy (37.72%), suggesting that explicit separation between positive and negative samples is crucial for data-scarce, high-resolution tasks.

Additional detailed figures including classification loss curves, layer-wise accuracy progression, and multi-pass accuracy analysis for all datasets are provided in the Appendix. For classification loss curves please refer to Figures 6, 7, 8, 9 in Appendix A.For layer-wise accuracy progression please refer to Figures 10, 11, 12, 13 in Appendix B. For multi-pass accuracy analysis for all datasets, please refer to Figures 14, 15, 16, 17 in Appendix C.

5 Discussion

In this work, we set out to explore the landscape of "goodness" functions for the Forward-Forward algorithm. Our benchmarking of 21 objectives across four datasets allows us to answer the research questions posed at the beginning of this study.

5.1 RQ1: Impact on Classification Accuracy

Our first question asked how the choice of goodness function impacts accuracy compared to the standard sum-of-squares baseline. The results unequivocally demonstrate that **minimizing prediction error and enforcing margins are superior to simple activity maximization.**

The predictive_coding_local function consistently outperformed (on classification accuracy) the baseline on almost all datasets including complex datasets like CIFAR-10, achieving a Multi-pass Accuracy of 43.42% compared to the baseline's 39.59%. This suggests that the standard Forward-Forward objective is insufficient for capturing the rich structure of natural images. By contrast, predictive coding forces the network to learn dependencies between neurons, aligning with theories of cortical function where the brain constantly attempts to predict its own states [43].

However, prediction is not the only path to goodness. On FashionMNIST, the softmax_energy_margin_local function achieved the highest Multi-pass Accuracy (86.32%), and on STL-10, triplet_margin_local led the pack (37.72%). This indicates that for fine-grained or data-scarce tasks, objectives that explicitly enforce separation between positive and negative samples, similar to contrastive learning margins which are highly effective in the Forward-Forward regime.

5.2 RQ2: Energy Consumption and Sustainability

Our second question investigated the variability in energy consumption and sought more sustainable alternatives. We found that the "carbon cost" of learning is highly sensitive to the specific mathematical operations used in the goodness function.

We identified whitened_energy_local and sparse_l1_local as the most sustainable alternatives. On FashionM-NIST, the whitened energy objective reduced carbon emissions by approximately 10% compared to the baseline (11.91 g vs 13.12 g) while maintaining competitive accuracy. This efficiency likely stems from the decorrelation of neural activities, which prevents redundant firing and allows the network to converge to a solution with fewer total synaptic updates. This finding supports the hypothesis that metabolically efficient learning rules such as those that favor sparse and decorrelated codes, and are naturally aligned with Green AI principles [44].

5.3 RQ3: Trade-offs and Pareto Optimality

Our final question asked if there is a trade-off between predictive performance and environmental efficiency. To answer this, we look for **Pareto-optimal** solutions, with choices where it is impossible to improve accuracy without increasing energy consumption, or vice versa.

Our analysis reveals distinct "sweet spots" on the Pareto frontier:

- 1. **The Performance Specialist:** For applications where accuracy is paramount, sparse_l1_local (CIFAR-10) and softmax_energy_margin_local (FashionMNIST) are the clear choices. Notably, sparse_l1_local dominates on CIFAR-10 by being both the most accurate and the most efficient.
- 2. **The Efficiency Specialist:** For resource-constrained environments, whitened_energy_local offers the best balance on simpler datasets like FashionMNIST. However, on complex data (CIFAR-10), sparse_11_local is the optimal choice for both performance and efficiency.

Crucially, the standard sum_of_squares baseline is often **sub-optimal**. In many cases, it is dominated by other functions that are either more accurate (like predictive coding) or more efficient (like whitened energy). This indicates that the default objective used in early Forward-Forward research is likely not the most effective choice for either performance or sustainability.

5.4 Limitations, Failure Modes and Conclusion

While many goodness functions demonstrated strong performance, we must acknowledge that certain objectives failed to learn meaningful representations. Specifically, functions like bcm_local and outlier_trimmed_energy_local occasionally reported accuracies around 10% (e.g., 9.86% for BCM on MNIST). Since these datasets contain 10 balanced classes, a 10% accuracy corresponds to random chance, indicating a complete failure of the learning process.

We hypothesize that these failures stem from the inherent instability of these objectives in a greedy, layer-wise training regime. The BCM rule, for instance, relies on a sliding threshold that is sensitive to the statistics of the input stream. Without the global error signal of backpropagation to correct for "runaway" updates, the threshold may fail to stabilize, leading to representational collapse where all neurons either saturate or die. Similarly, outlier trimming can be too aggressive, discarding useful signal as noise. These results highlight a critical limitation of biologically plausible local learning: it requires careful hyperparameter tuning and homeostatic mechanisms to maintain stability, which global optimization methods often take for granted.

To conclude, the "search for goodness" reveals that the objective function is a powerful lever for shaping both the intelligence and the efficiency of biologically plausible networks. By moving beyond simple activity maximization and embracing principles of prediction, sparsity, and margins, we can build Forward-Forward networks that are not only smarter but also greener. Future work should extend this analysis to neuromorphic hardware, where the local nature of these rules could yield even greater efficiency gains [45].

Acknowledgments

We acknowledge National Supercomputing Mission (NSM) for providing computing resources of 'PARAM Ananta' at IIT Gandhinagar, which is implemented by C-DAC and supported by the Ministry of Electronics and Information Technology (MeitY) and Department of Science and Technology (DST), Government of India.

References

- [1] David E Rumelhart, Geoffrey E Hinton, and Ronald J Williams. Learning representations by back-propagating errors. *Nature*, 323(6088):533–536, October 1986.
- [2] F Crick. The recent excitement about neural networks. *Nature*, 337(6203):129–132, January 1989.

- [3] Yoshua Bengio, Dong-Hyun Lee, Jorg Bornschein, Thomas Mesnard, and Zhouhan Lin. Towards biologically plausible deep learning, 2016.
- [4] Timothy P Lillicrap, Adam Santoro, Luke Marris, Colin J Akerman, and Geoffrey Hinton. Backpropagation and the brain. *Nat. Rev. Neurosci.*, 21(6):335–346, June 2020.
- [5] James C R Whittington and Rafal Bogacz. Theories of error back-propagation in the brain. *Trends Cogn. Sci.*, 23(3):235–250, March 2019.
- [6] Timothy P Lillicrap, Daniel Cownden, Douglas B Tweed, and Colin J Akerman. Random synaptic feedback weights support error backpropagation for deep learning. *Nat. Commun.*, 7(1):13276, November 2016.
- [7] Benjamin Scellier and Yoshua Bengio. Equilibrium propagation: Bridging the gap between energy-based models and backpropagation. *Front. Comput. Neurosci.*, 11:24, May 2017.
- [8] R P Rao and D H Ballard. Predictive coding in the visual cortex: a functional interpretation of some extra-classical receptive-field effects. *Nat. Neurosci.*, 2(1):79–87, January 1999.
- [9] Geoffrey Hinton. The forward-forward algorithm: Some preliminary investigations, 2022.
- [10] Ting Chen, Simon Kornblith, Mohammad Norouzi, and Geoffrey Hinton. A simple framework for contrastive learning of visual representations, 2020.
- [11] Kaiming He, Haoqi Fan, Yuxin Wu, Saining Xie, and Ross Girshick. Momentum contrast for unsupervised visual representation learning, 2020.
- [12] Aaron van den Oord, Yazhe Li, and Oriol Vinyals. Representation learning with contrastive predictive coding, 2019.
- [13] Emma Strubell, Ananya Ganesh, and Andrew McCallum. Energy and policy considerations for deep learning in nlp, 2019.
- [14] Roy Schwartz, Jesse Dodge, Noah A Smith, and Oren Etzioni. Green AI. Commun. ACM, 63(12):54–63, November 2020.
- [15] David Patterson, Joseph Gonzalez, Quoc Le, Chen Liang, Lluis-Miquel Munguia, Daniel Rothchild, David So, Maud Texier, and Jeff Dean. Carbon emissions and large neural network training, 2021.
- [16] D. O. Hebb. *The organization of behavior; a neuropsychological theory.* The organization of behavior; a neuropsychological theory. Wiley, Oxford, England, 1949.
- [17] Erkki Oja. Simplified neuron model as a principal component analyzer. *J. Math. Biol.*, 15(3):267–273, November 1982.
- [18] E L Bienenstock, L N Cooper, and P W Munro. Theory for the development of neuron selectivity: orientation specificity and binocular interaction in visual cortex. *J. Neurosci.*, 2(1):32–48, January 1982.
- [19] Yoshua Bengio. How auto-encoders could provide credit assignment in deep networks via target propagation, 2014.
- [20] Dong-Hyun Lee, Saizheng Zhang, Asja Fischer, and Yoshua Bengio. Difference target propagation, 2015.
- [21] Max Jaderberg, Wojciech Marian Czarnecki, Simon Osindero, Oriol Vinyals, Alex Graves, David Silver, and Koray Kavukcuoglu. Decoupled neural interfaces using synthetic gradients, 2017.
- [22] Yann LeCun, Sumit Chopra, Raia Hadsell, Aurelio Ranzato, and Fu Jie Huang. A tutorial on energy-based learning, 2006.
- [23] J J Hopfield. Neural networks and physical systems with emergent collective computational abilities. *Proc. Natl. Acad. Sci. U. S. A.*, 79(8):2554–2558, April 1982.
- [24] Geoffrey E. Hinton and Terrence J. Sejnowski. Optimal perceptual inference. In *Proceedings of the IEEE Conference on Computer Vision and Pattern Recognition*, 1983.
- [25] Geoffrey E Hinton. Training products of experts by minimizing contrastive divergence. *Neural Comput.*, 14(8):1771–1800, August 2002.
- [26] Aapo Hyvärinen. Estimation of non-normalized statistical models by score matching. *Journal of Machine Learning Research*, 6(24):695–709, 2005.
- [27] Jean-Bastien Grill, Florian Strub, Florent Altché, Corentin Tallec, Pierre Richemond, Elena Buchatskaya, Carl Doersch, Bernardo Avila Pires, Zhaohan Guo, Mohammad Gheshlaghi Azar, Bilal Piot, koray kavukcuoglu, Remi Munos, and Michal Valko. Bootstrap your own latent a new approach to self-supervised learning. In H. Larochelle, M. Ranzato, R. Hadsell, M.F. Balcan, and H. Lin, editors, *Advances in Neural Information Processing Systems*, volume 33, pages 21271–21284. Curran Associates, Inc., 2020.

- [28] Xinlei Chen and Kaiming He. Exploring simple siamese representation learning, 2020.
- [29] Jure Zbontar, Li Jing, Ishan Misra, Yann LeCun, and Stéphane Deny. Barlow twins: Self-supervised learning via redundancy reduction, 2021.
- [30] Mathilde Caron, Ishan Misra, Julien Mairal, Priya Goyal, Piotr Bojanowski, and Armand Joulin. Unsupervised learning of visual features by contrasting cluster assignments, 2021.
- [31] Florian Schroff, Dmitry Kalenichenko, and James Philbin. Facenet: A unified embedding for face recognition and clustering. In 2015 IEEE Conference on Computer Vision and Pattern Recognition (CVPR), page 815–823. IEEE, June 2015.
- [32] Michael Cogswell, Faruk Ahmed, Ross Girshick, Larry Zitnick, and Dhruv Batra. Reducing overfitting in deep networks by decorrelating representations, 2016.
- [33] David Balduzzi, Sebastien Racaniere, James Martens, Jakob Foerster, Karl Tuyls, and Thore Graepel. The mechanics of n-player differentiable games, 2018.
- [34] M J Kirkby. The fractal geometry of nature. benoit b. mandelbrot. w. h. freeman and co., san francisco, 1982. no. of pages: 460. price: £22.75 (hardback). *Earth Surf. Process.*, 8(4):406–406, July 1983.
- [35] Peter J Huber. Robust estimation of a location parameter. In *Springer Series in Statistics*, Springer series in statistics, pages 492–518. Springer New York, New York, NY, 1992.
- [36] Peter J Rousseeuw. Least median of squares regression. J. Am. Stat. Assoc., 79(388):871, December 1984.
- [37] Weiyang Liu, Yandong Wen, Zhiding Yu, and Meng Yang. Large-margin softmax loss for convolutional neural networks, 2017.
- [38] A Hyvärinen and E Oja. Independent component analysis: algorithms and applications. *Neural Netw.*, 13(4-5):411–430, May 2000.
- [39] B A Olshausen and D J Field. Emergence of simple-cell receptive field properties by learning a sparse code for natural images. *Nature*, 381(6583):607–609, June 1996.
- [40] Ashish Vaswani, Noam Shazeer, Niki Parmar, Jakob Uszkoreit, Llion Jones, Aidan N. Gomez, Lukasz Kaiser, and Illia Polosukhin. Attention is all you need, 2023.
- [41] David Broomhead and David Lowe. Radial basis functions, multi-variable functional interpolation and adaptive networks. ROYAL SIGNALS AND RADAR ESTABLISHMENT MALVERN (UNITED KINGDOM), RSRE-MEMO-4148, 03 1988.
- [42] Benoît Courty, Victor Schmidt, Goyal-Kamal, inimaz, MarionCoutarel, Luis Blanche, Boris Feld, Jérémy Lecourt, LiamConnell, Amine Saboni, SabAmine, supatomic, Patrick Lloret, Mathilde Léval, Alexis Cruveiller, ouminasara, Franklin Zhao, Christian Bauer, Aditya Joshi, Jerry Laruba Festus, Alexis Bogroff, Niko Laskaris, Hugues de Lavoreille, Alexandre Phiev, Edoardo Abati, Douglas Blank, rosekelly, and cianc. mlco2/codecarbon: v3.1.0, 2025.
- [43] Karl Friston. The free-energy principle: a unified brain theory? *Nat. Rev. Neurosci.*, 11(2):127–138, February 2010.
- [44] Simon B Laughlin and Terrence J Sejnowski. Communication in neuronal networks. *Science*, 301(5641):1870–1874, September 2003.
- [45] Mike Davies, Narayan Srinivasa, Tsung-Han Lin, Gautham Chinya, Yongqiang Cao, Sri Harsha Choday, Georgios Dimou, Prasad Joshi, Nabil Imam, Shweta Jain, Yuyun Liao, Chit-Kwan Lin, Andrew Lines, Ruokun Liu, Deepak Mathaikutty, Steven McCoy, Arnab Paul, Jonathan Tse, Guruguhanathan Venkataramanan, Yi-Hsin Weng, Andreas Wild, Yoonseok Yang, and Hong Wang. Loihi: A neuromorphic manycore processor with on-chip learning. *IEEE Micro*, 38(1):82–99, 2018.

A Appendix A. Per Dataset Classification Loss Plots

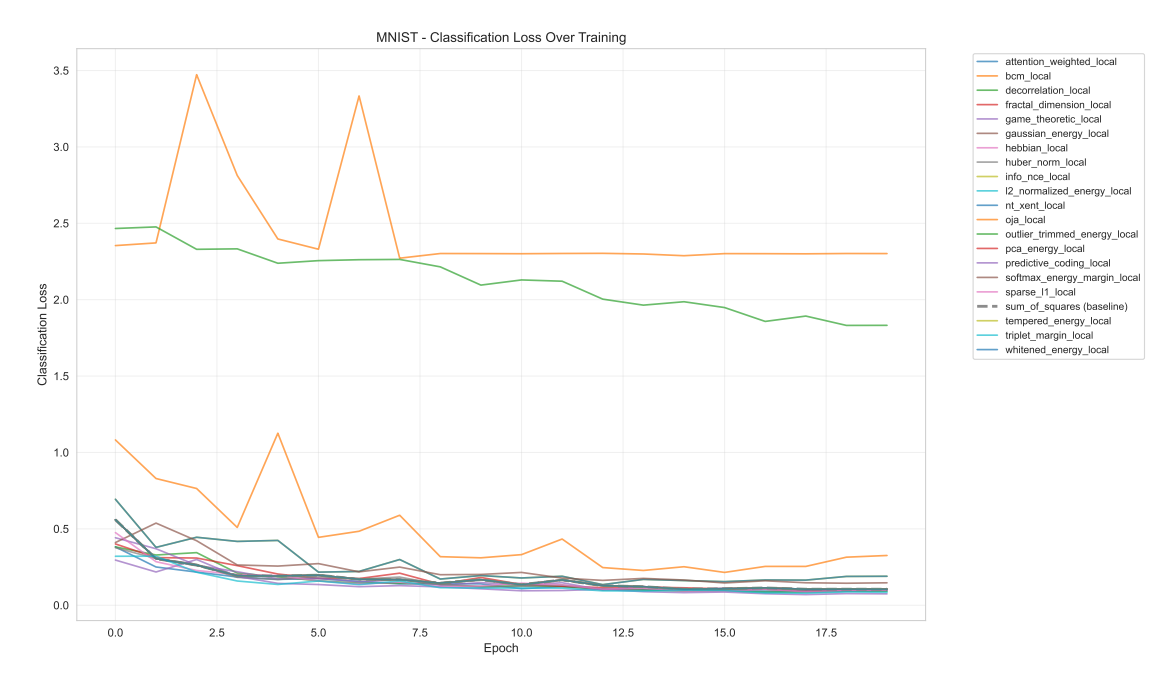


Figure 6: Classification Loss over training epochs on the MNIST dataset. Most functions converge rapidly to a low loss, while unstable functions like bcm_local exhibit high, fluctuating loss values.

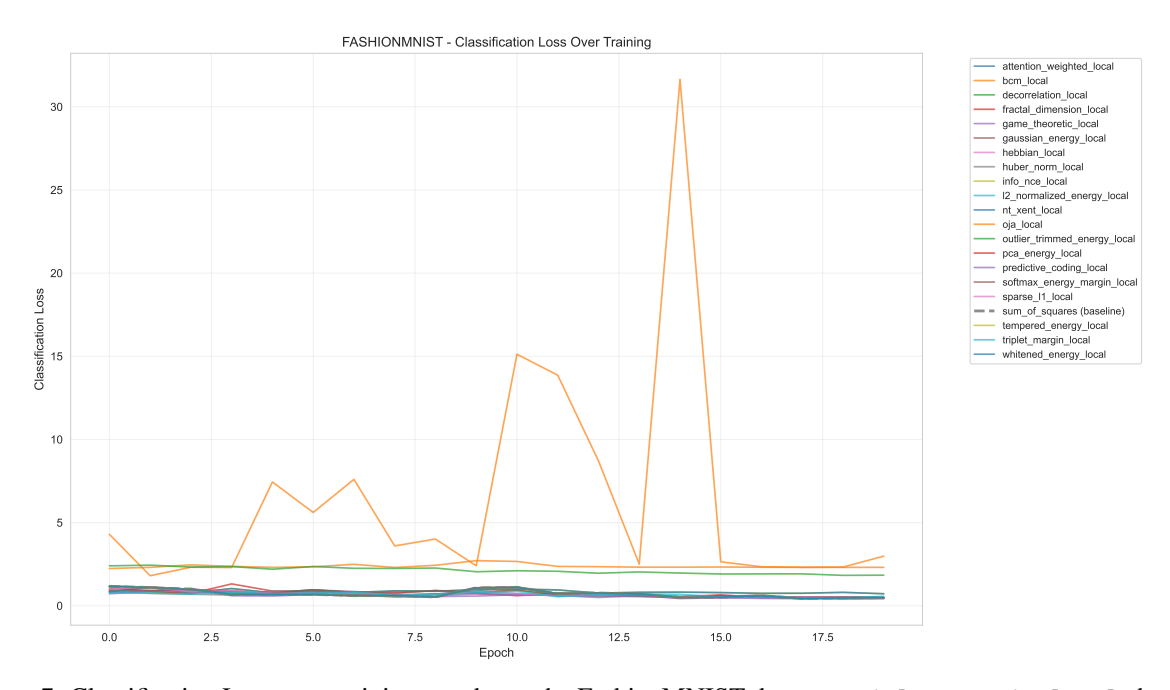


Figure 7: Classification Loss over training epochs on the FashionMNIST dataset. triplet_margin_local shows a distinct spike in loss during mid-training before converging.

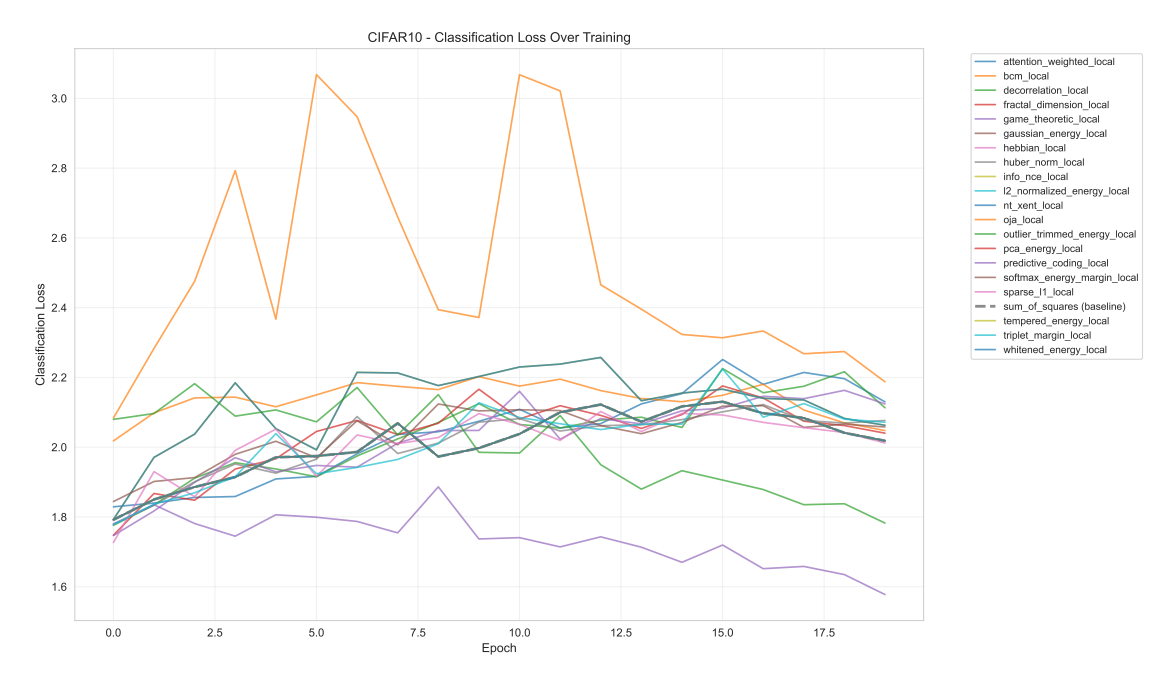


Figure 8: Classification Loss over training epochs on the CIFAR-10 dataset. The loss curves exhibit more variance compared to MNIST, reflecting the higher complexity of the dataset.

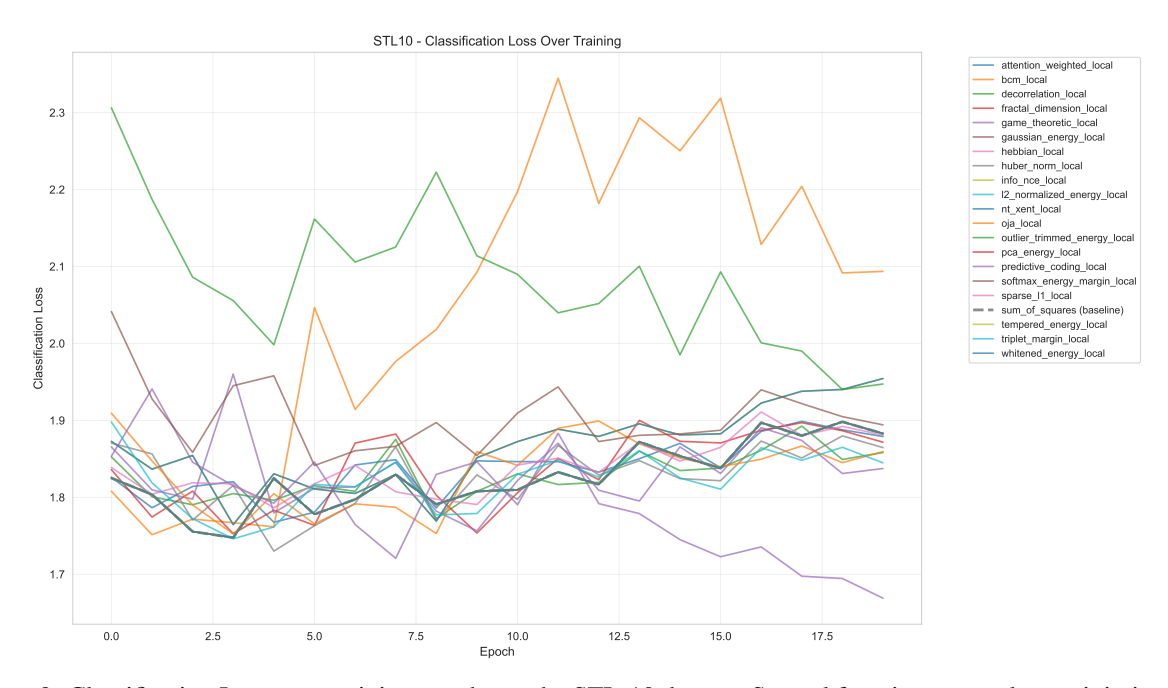


Figure 9: Classification Loss over training epochs on the STL-10 dataset. Several functions struggle to minimize loss consistently, indicated by jagged and non-converging lines.

B Appendix B. Per Dataset Accuracy Per Layer Plots

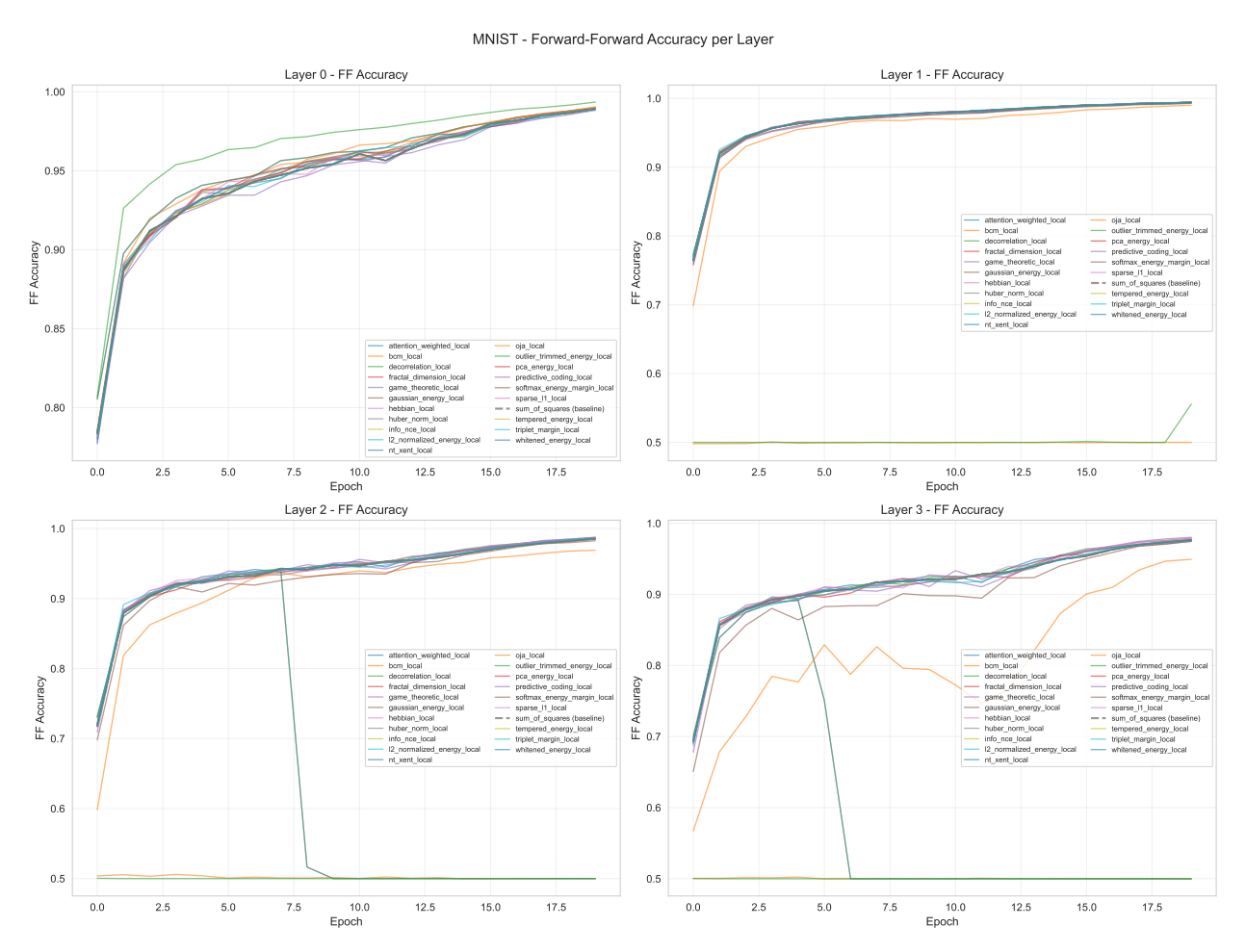


Figure 10: Forward-Forward Accuracy per Layer on MNIST. Panels display the accuracy progression for Layer 0 through Layer 3. Deeper layers generally maintain high accuracy, though some functions show degradation in Layer 3.

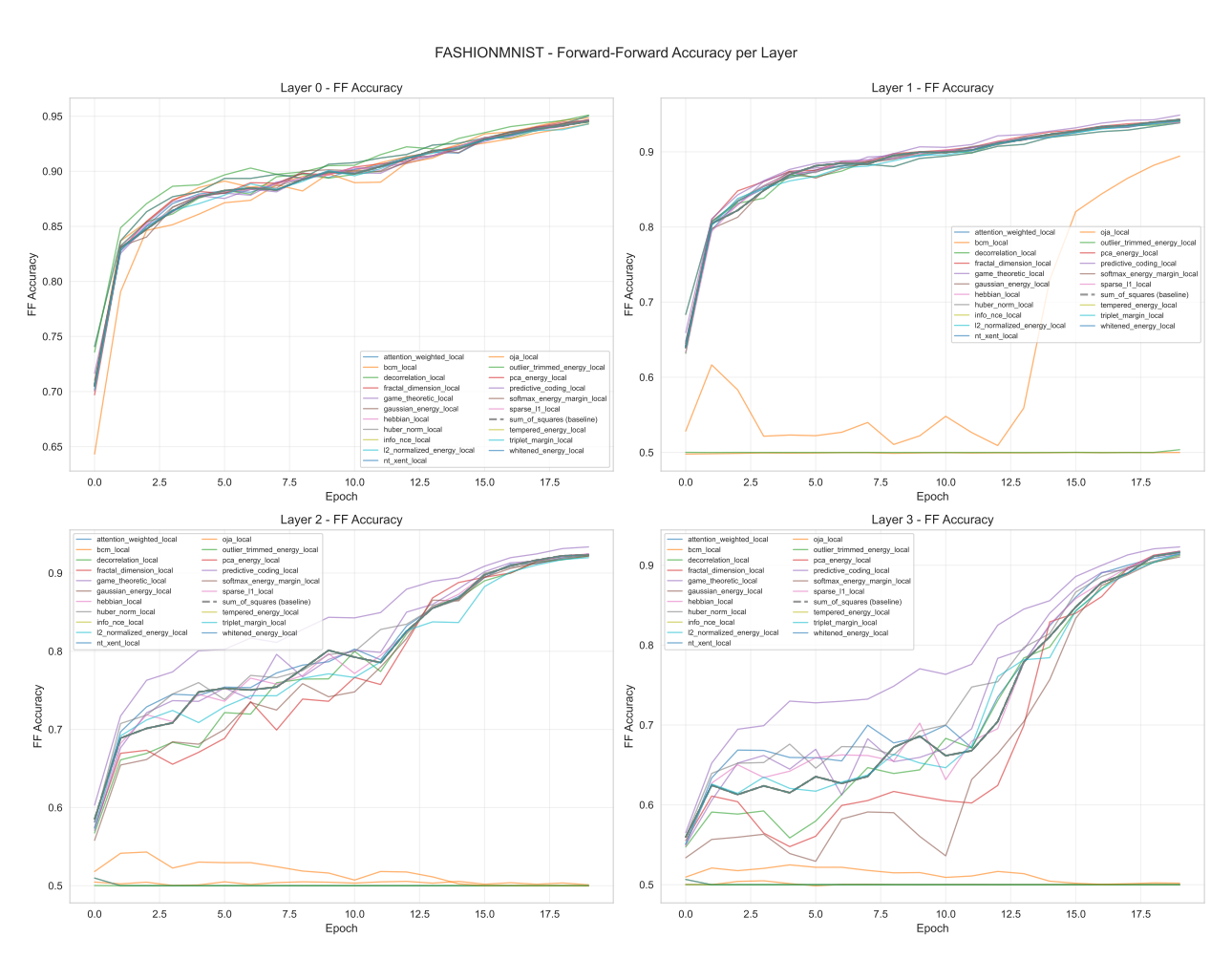


Figure 11: Forward-Forward Accuracy per Layer on FashionMNIST. Accuracy tends to increase in deeper layers for top-performing functions, while unstable functions fail to improve after the first layer.

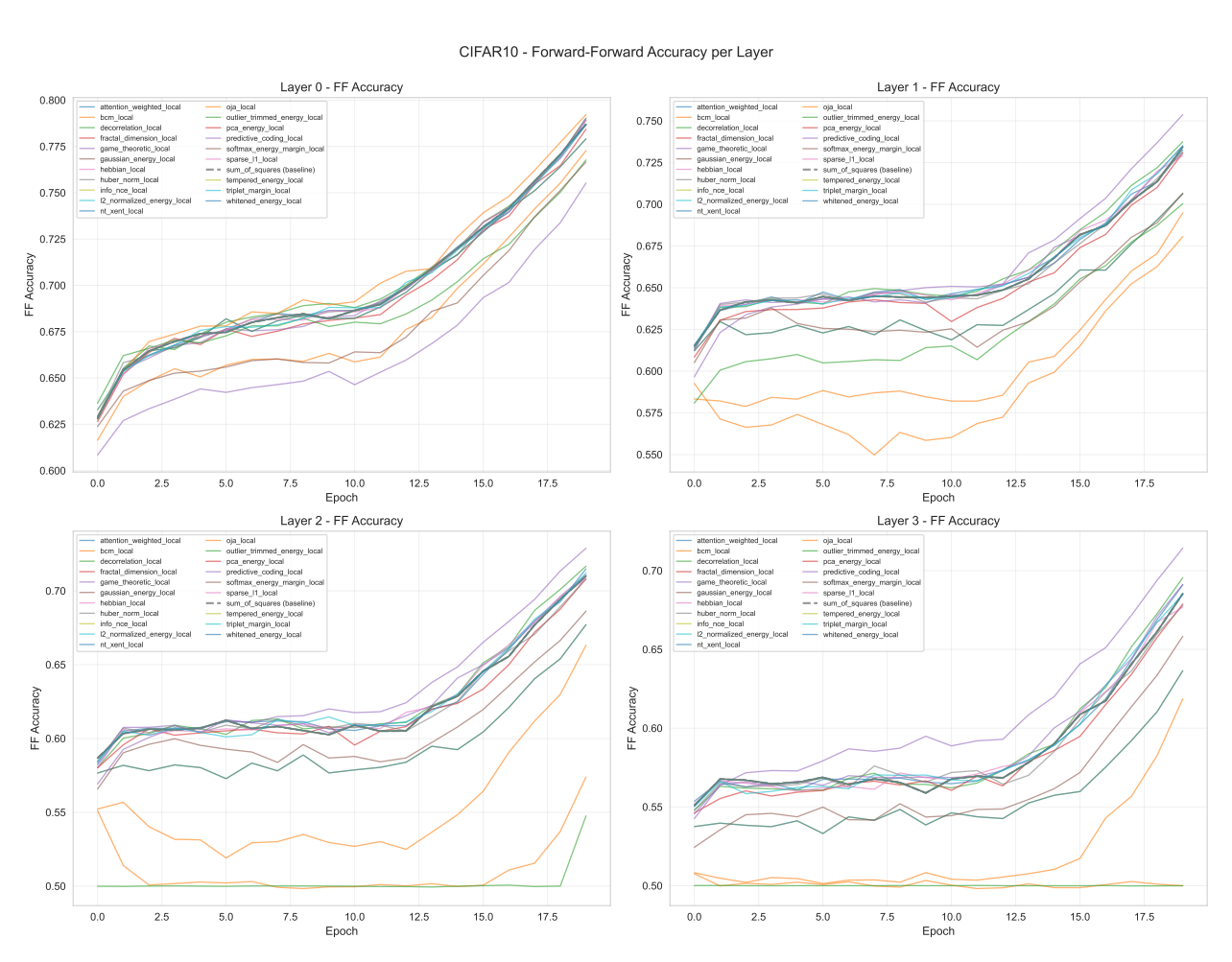


Figure 12: Forward-Forward Accuracy per Layer on CIFAR-10. The gap between high-performing functions (like predictive coding) and baselines becomes more pronounced in deeper network layers.



Figure 13: Forward-Forward Accuracy per Layer on STL-10. Accuracy progression is slower and more variable compared to simpler datasets, highlighting the difficulty of the task.

C Appendix C. Per Dataset Multi-pass Accuracy Plots

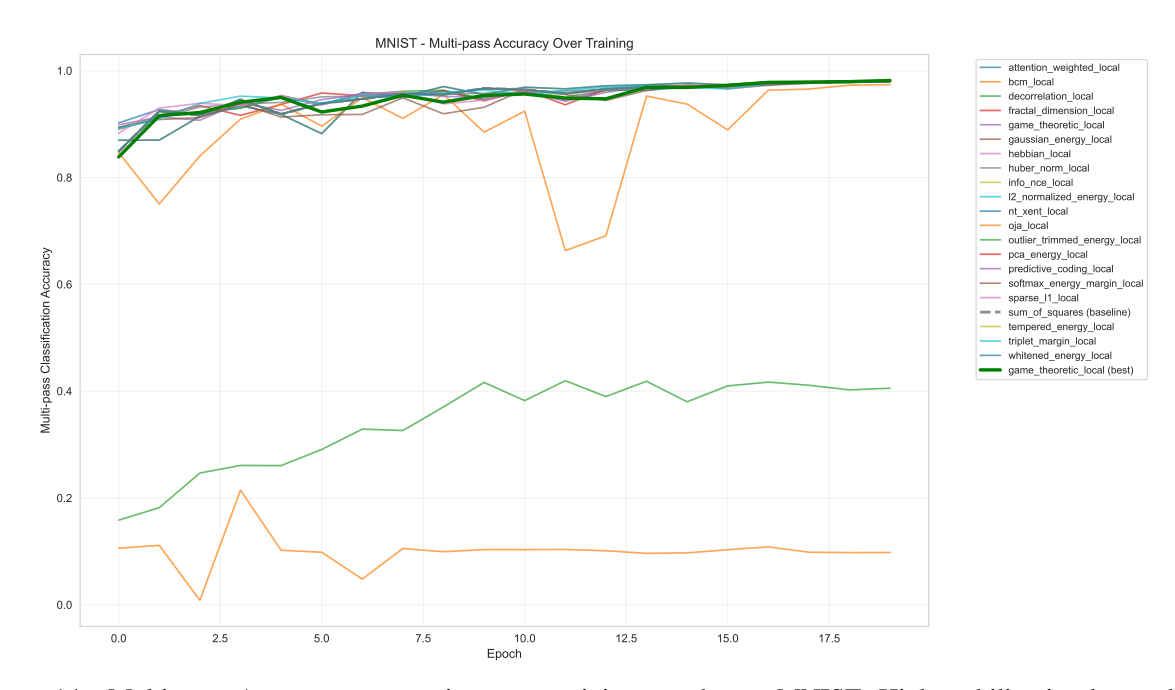


Figure 14: Multi-pass Accuracy progression over training epochs on MNIST. High stability is observed for game_theoretic_local (green line).

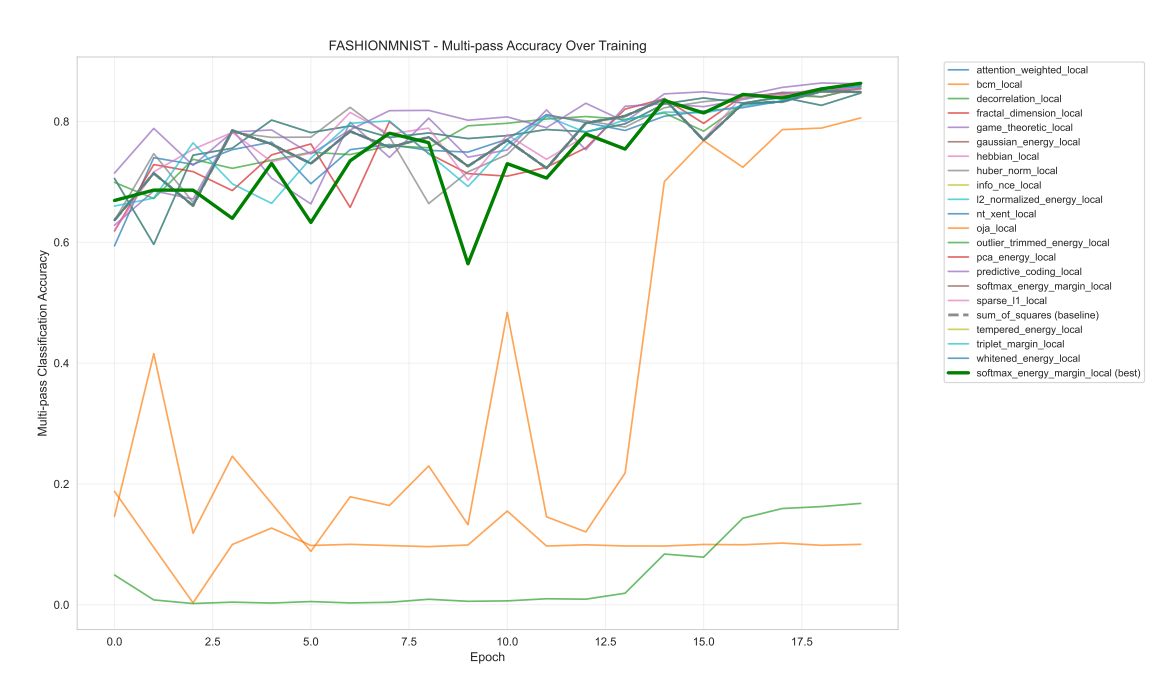


Figure 15: Multi-pass Accuracy progression over training epochs on FashionMNIST. The softmax_energy_margin_local function (highlighted green) demonstrates consistent improvement and stability.

23

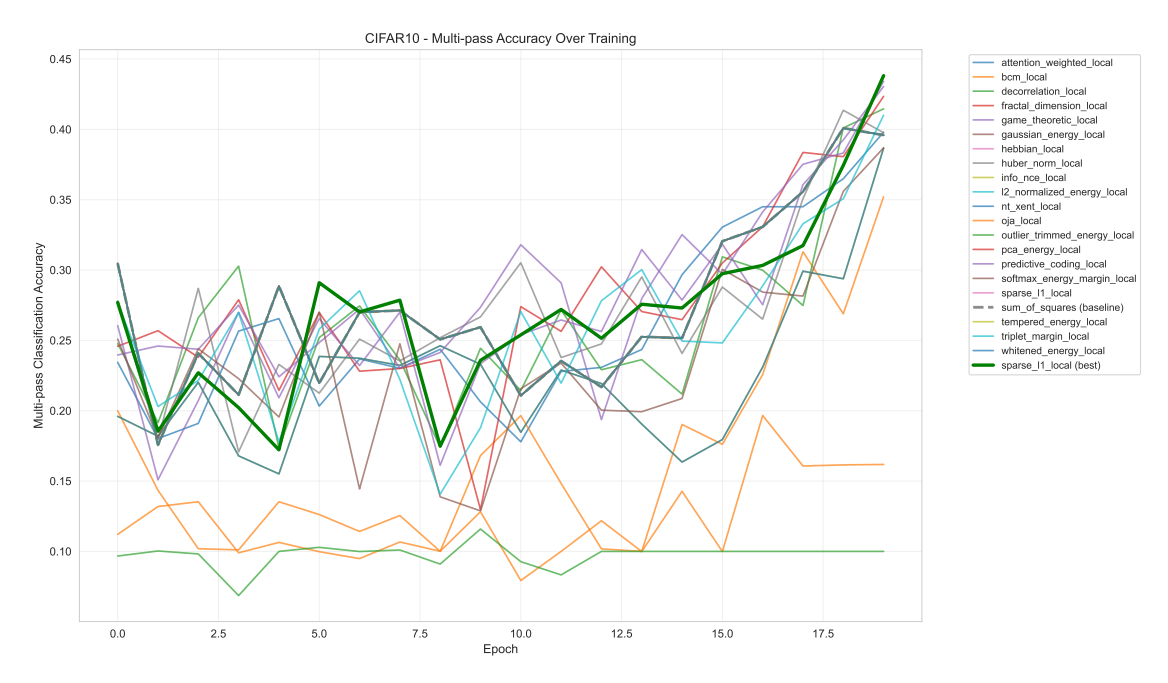


Figure 16: Multi-pass Accuracy progression over training epochs on CIFAR-10. sparse_11_local (green line) shows a steady upward trend, outperforming the baseline.

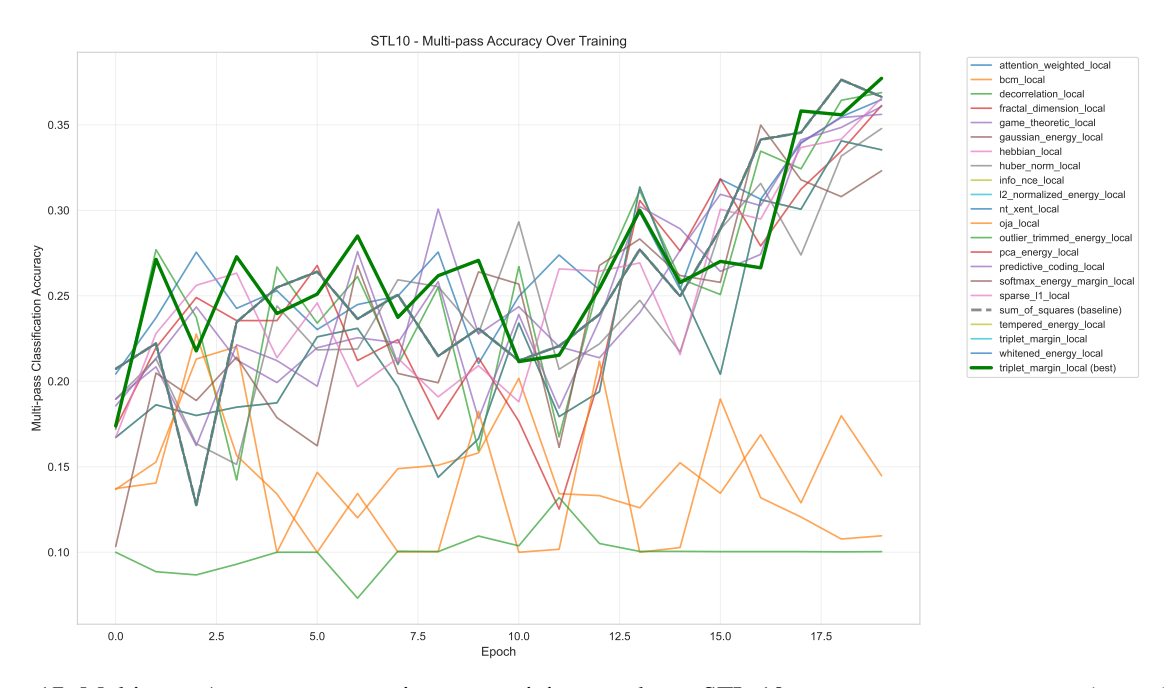


Figure 17: Multi-pass Accuracy progression over training epochs on STL-10. triplet_margin_local (green line) demonstrates superior convergence characteristics compared to other functions.